KSCE Journal of Civil Engineering (2013) 17(7):1690-1699

DOI 10.1007/s12205-013-0463-1

Structural Engineering

pISSN 1226-7988, eISSN 1976-3808
www.springer.com/12205

Shape Optimization of Arch Dams under Earthquake Loading using Meta-Heuristic Algorithms

A. Kaveh* and V. R. Mahdavi**

Received September 9, 2012/Accepted January 24, 2013

Abstract

This paper presents efficiency of three meta-heuristic algorithms for large-scale shape optimization of double curvature arch dams under seismic loading condition with different constraints such as failure, stability and geometrical limitations. The earthquake load is considered by time variant ground acceleration applied in the upstream–downstream direction of the arch dam. Here, the Westergaard method is used to include the dam-reservoir interaction. For optimization, the Charged System Search (CSS), Particle Swarm Optimization (PSO), and a hybrid CSS and PSO (CSS-PSO) are utilized. Numerical results demonstrate the effectiveness of the meta-heuristic algorithms for optimal shape design of arch dams. Comparative studies illustrates that the superiority CSS-PSO algorithm compared to the standard PSO and CSS. A parametric study is also conducted to investigate the effect of water depth and earthquake intensity on the cost optimization of the arch dams.

Keywords: *optimal design, arch dams, charged system search algorithm, particle swarm optimization, hybrid method*

1. Introduction

Arch dam optimization is one of the most active fields of research in structural optimization. Generally, in design optimization of arch dams, the objective is to find the best feasible shape of arch dam with a minimum weight or construction cost. In other words, optimum design of arch dams is a search for the best possible arrangements of design variables according to the determined constrains.

The shape optimization of arch dams has been developed after appearing and development of finite element method in late 1950's. Early research works dealt mainly with membrane-type solutions, Fialho (1955). Later, Rajan (1968), Mohr (1979) and Sharma (1983) developed solutions based on membrane shell theory. Sharpe (1969) was the first to formulate the optimization as a mathematical programming problem. A similar method was also adopted by Rickeetts and Zienkiewicz (1975) who used finite element method for stress analysis and Sequential Linear Programming (SLP) for the shape optimization of arch dams under static loading.

Recently, a novel meta-heuristic algorithm known as Charged System Search (CSS) was introduced by Kaveh and Talatahari (2010a, b, c), and applied to different engineering optimization problems. The CSS utilizes the Coulomb and Gauss's laws from electrostatics, and the Newtonian laws of mechanics. Particle Swarm Optimization (PSO) is another meta-heuristic algorithm widely utilized for optimization problems due to its simple principle and ease of implementation, Eberhart and Kennedy (1995). Kaveh and Talatahari (2011) have utilized a new methodology based on the combination of the CSS and PSO.

In this study, three meta-heuristic mentioned algorithms are employed for cost and volume optimization of arch dams. The construction cost of dam consisting of the concrete volume and the casting areas is considered as the objective function. To implement a practical design optimization, many constraints such as stress, displacement, stability requirement, and frequency constraints should be considered. In the present study, for simplicity of the optimization operation, stress and some geometrical constraints are considered. The inertia forces of the impounded water are represented by added hydrodynamic mass values in accordance with the generalized Westergaard (1933) method. The Opensees (2003) is used for modeling and time history analysis. Moreover, the optimization procedure requiring, among other things, the calculation of volume and cost of the arch dam, is implemented in Matlab (2009). Two examples of large-scale arch dams to be designed for minimum volume and cost are considered in order to demonstrate the capability of the meta-heuristic algorithms in solving large-scale arch dam optimization problems. In the final section, parametric study is performed to show the effect of different parameters (the water depths and earthquake intensity)

*Professor, Centre of Excellence for Fundamental Studies in Structural Engineering, Iran University of Science and Technology, Narmak, Tehran-16, Iran (Corresponding Author, E-mail: alikaveh@iust.ac.ir)
**Ph.D. Student, School of Civil Engineering, Iran University of Science and Technology, Narmak, Tehran-16, Iran (E-mail: vahidreza_mahdavi@civileng.iust.ac.ir)

in the cost optimization of the arch dams.

2. Optimization Algorithms

Methods employed in structural optimization design problems can be divided into mathematical programming and meta-heuristic algorithms. Due to the difficulties encountered in mathematical programming (complex derivatives, sensitivity to initial values, and the large amount of enumeration memory required) for complex problems, various kinds of meta-heuristic algorithms have been developed for optimum design of structures. As stated before, in this paper, three powerful advanced algorithms consisting of the standard CSS, the standard PSO and CSS-PSO are employed for optimal design of arch dams.

2.1 The Standard Charged Search System

The Charged System Search, developed by Kaveh and Talatahari (2010a), is a population-based search approach which is based on principles from physics and mechanics. In this approach each agent is a solid particle (CP) of radius “a” which is considered as a charged sphere of radius a, having a uniform volume charge density that can produce an electric force on the other CPs. The force magnitude for a CP located inside the sphere is proportional to the separation distance between the CPs, while for a CP located outside the sphere it is inversely proportional to the square of the separation distance between the particles. The resultant forces or acceleration and the motion laws determine the new location of the CPs. The pseudo-code for the CSS algorithm can be summarized as follows (Kaveh and Talatahari, 2010b, c):

Step 1: *Initialization.* The initial positions of CPs are determined randomly in the search space and the initial velocities of charged particles are assumed to be zero. The values of the fitness function for the CPs are determined and the CPs are sorted in an increasing order. A number of the first CPs and their related values of the fitness function are saved in a memory, so called Charged Memory (CM).

Step 2: *Determination of the forces on CPs.* The force vector is calculated for jth CP as:

$$F_j = \sum_{i=1}^{N} \langle \frac{q_i}{a^3} r_{i,j}.i_1 + \frac{q_i}{r_{i,j}}.i_2 \rangle ar_{i,j} P_{i,j}(X_i - X_j) < \begin{array}{l} j = 1,2,\ldots,N \\ i_1 = 1, i_2 = 0 \quad if \quad r_{i,j} < a \\ i_1 = 0, i_2 = 1 \quad if \quad r_{i,j} \geq a \end{array} \tag{1}$$

where F_j is the resultant force acting on the jth CP; X_i and X_j are the position vectors of the ith and jth CPs, respectively, Here a is the radius of the charged sphere and N is the number of CPs. The magnitude of charge for each CP (q_i) is defined considering the quality of its solution as:

$$q_i = \frac{fit(i) - fitwrost}{fitbest - fitwrost}, \quad i = 1,2,\ldots,N \tag{2}$$

where *fitbest* and *fitworst* are the best and the worst fitness of all particles, respectively; *fit*(i) represents the fitness of the agent i; and N is the total number of CPs. The separation distance $r_{i,j}$ between two charged particles is defined as follows:

$$r_{i,j} = \frac{\|X_i - X_j\|}{\|(X_i + X_j)/2 - X_{best}\| + \varepsilon} \tag{3}$$

where X_{best} is the position of the best current CP, and ε is a small positive number. Here, $p_{i,j}$ is the probability of moving each CP towards the others and is obtained using the following function:

$$P_{i,j} = \begin{cases} 1 & \frac{fit(i) - fitbest}{fit(j) - fit(i)} > rand \wedge fit(j) > fit(i) \\ 0 & else \end{cases} \tag{4}$$

In Eq. (1), $ar_{i,j}$ indicates the kind of force and is defined as:

$$ar_{i,j} = \begin{cases} +1 & rand < 0.8 \\ -1 & else \end{cases} \tag{5}$$

where *rand* represents a random number.

Step 3: *Solution construction.* Each CP moves to the new position and the new velocity is calculated as:

$$X_{j,news} = rand_{j,1}.K_a.F_j + rand_{j,1}.K_v.V_{j,old} + X_{j,old} \tag{6}$$

$$V_{j,new} = X_{j,new} - X_{j,old} \tag{7}$$

where K_a is the acceleration coefficient; K_v is the velocity coefficient to control the influence of the previous velocity; and $rand_{j,1}$ and $rand_{j,2}$ are two random numbers uniformly distributed in the range (0,1). In this paper K_v and K_a are taken as:

$$K_a = 0.5\left(1 + \frac{iter}{iter_{\max}}\right), K_v = 0.5\left(1 - \frac{iter}{iter_{\max}}\right) \tag{8}$$

iter is the iteration number and $iter_{\max}$ is the maximum number of iterations.

Step 4: *Updating process.* If a new CP exits from the allowable search space, a harmony search-based handling approach is used to correct its position (Kaveh and Talatahari, 2010a). In addition, if some new CP vectors are better than the worst ones in the CM, these are replaced by the worst ones in the CM.

Step 5: *Termination criterion control.* Steps 2-4 are repeated until a termination criterion is satisfied (Kaveh and Talatahari, 2010a, b, c).

2.2 The Particle Swarm Optimization

The PSO is based on a metaphor of social interaction such as bird flocking and fish schooling, and is developed by Eberhart and Kennedy (1995). The PSO simulates a commonly observed social behavior, where members (particles) of a group (swarm) tend to follow the lead of the best of the group. In other words, the particles fly through the search space and their positions are updated based on the best positions of individual particles denoted by p_i^k and the best position among all particles in the search space represented by p_g^k.

The procedure of the PSO is reviewed below:

Step 1: Initialization. An array of particles and their associated velocities are initialized with random positions.

Step 2: Local and global best creation. The initial particles are considered as the first local best and the best of them corresponding to the minimum objective function will be the first global best.

Step 3: Solution construction. The location of each particle is changed to the new position using the following equations:

$$X_i^{k+1} = X_i^k + \omega V_i^k + C_1 r_1 \circ (P_i^k - X_i^k) + C_2 r_2 \circ (P_g^k - X_i^k) \tag{9}$$

Where X_i^k and V_i^k are the position and velocity for the ith particle at iteration k; ω is an inertia weight to control the influence of the previous velocity; r_1, and r_2 are two random numbers uniformly distributed in the range of (0, 1); C_1 and C_2 are two acceleration constants; P_i^k is the best position of the ith particle up to iteration k; P_g^k is the best position among all particles in the swarm up to iteration k and the sign "∘" denotes element-by-element multiplication.

In this paper ω is taken as:

$$\omega = 0.8\left(1 - 0.5\frac{iter}{iter_{\max}}\right) \tag{10}$$

$iter$ is the iteration number and $iter_{\max}$ is the maximum number of iterations.

Step 4: Local best updating. The objective function of the particles is evaluated and P_i^k is updated according to the best current value of the fitness function.

Step 5: Global best updating. The current global minimum objective function value among the current positions is determined and thus P_g^k is updated if the new position is better than the previous one.

Step 6: Terminating criterion control. Step 3 to Step 5 are repeated until a terminating criterion is satisfied (Kaveh and Talatahari, 2010c).

2.3 Hybrid Charged System Search and Particle Swarm Optimization

The Particle Swarm Optimization (PSO) utilizes a velocity term which is a combination of the previous velocity, V_i^k, the movement in the direction of the local best, P_i^k, the movement in the direction of the global best, P_g^k. In the present hybrid algorithm (Kaveh and Talatahari, 2011), the advantage of the PSO consisting of utilizing the local best and the global best is added to the CSS algorithm. The Charged Memory (CM) for the hybrid algorithm is treated as the local best in the PSO, and the CM updating process is defined as follows:

$$CM_{i,new} = \begin{cases} CM_{i,old} & W(X_{i,new}) \geq W(X_{i,old}) \\ X_{i,new} & W(X_{i,new}) < W(X_{i,old}) \end{cases} \tag{11}$$

in which the first term identifies that when the new position is not better than the previous one, the updating will not be performed, while when the new position is better than the so far stored good position, the new solution vector is replaced. Considering the above mentioned new charged memory, the resultant forces generated by agents are modified as:

$$F_j = c_1(CM_{g,old} - X_j) + c_2(CM_{j,old} - X_j) + \sum_{i \in s_1} k_i(CM_{i,old} - X_j) + \sum_{i \in s_2} K_i(X_i - X_j) \tag{12}$$

where c_1 and c_2 (similar to standard PSO) are user defined coefficient. The subtitle g denotes the number of the stored so far good position among all CPs. Therefore the first term directs the agents towards the global best position. When $i = j$, then the $CM_{i,old}$ is treated similar to P_i^k in the PSO as considered in the second term of the above equation. This will direct the agents towards the local best. The sets S_1 and S_2 are defined as follows:

$$S_1 = \{t_1, t_2, \ldots, t_n | q(t) > q(j), j = 1, 2, \ldots, N, j \neq i, g\}$$
$$S_2 = S - S_1 \tag{13}$$

where S_1 defines a set of n agents taken from CM and utilized in Eq. (11). If the set S includes all agents, the set S_2 will be the set of currently updated agents used to direct agent j. In addition, in the early optimization cycles, n is set to zero and is then linearly increased to N towards the end of the optimization process. The coefficient K_i is defined as:

$$K_i = \left(\frac{q_i}{a^3} r_{ij}.i_1 + \frac{q_i}{r^2}.i_2\right) ar_{ij} p_{ij} \tag{14}$$

3. Geometrical Model of an Arch Dam

3.1 Shape of the Central Vertical Section

The shape of a double-curvature arch dam has two basic characteristics: curvature and thickness. Both the curvature and the thickness change in horizontal and vertical directions. For the central vertical section of double-curvature arch dam, as shown in Fig. 1, one polynomial of nth order is used to determine the curve of upstream boundary and another polynomial is employed to determine the thickness. In this study, a parabolic function is considered for the curve of upstream face as (Gholizadeh and Seyedpoor, 2011):

$$y(z) = b(z) = -sz + \frac{sz^2}{2\beta h} \tag{15}$$

where h and s are the height of the dam and the slope at crest respectively, and the point where the slope of the upstream face

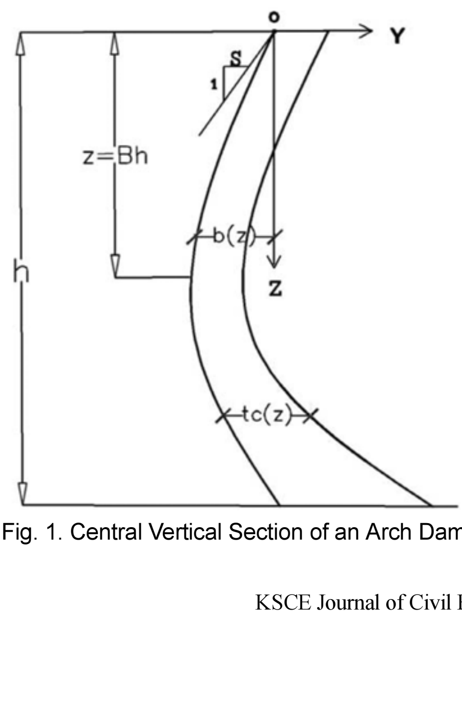

Fig. 1. Central Vertical Section of an Arch Dam

equals to zero is $z = \beta h$ in which β is constant.

By dividing the height of dam into n equal segments containing $n+1$ levels, the thickness of the central vertical section can be expressed as:

$$t_c(z) = \sum_{i=1}^{n+1} L_i(z) t_{ci} \tag{16}$$

in which, t_{ci} is the thickness of the central vertical section at the ith level. Also, in the above relation $L_i(z)$ is a Lagrange interpolation function associated with the ith level and can be defined as:

$$L_i(z) = \frac{\Pi_{K=1}^{n+1}(Z-Z_k)}{\Pi_{K=1}^{n+1}(Z-Z_k)} \qquad i \neq k \tag{17}$$

where z_i and z_k denotes the z coordinate of the ith and kth level in the central vertical section, respectively.

3.2 Shape of the Horizontal Section

As shown in Fig. 2, for the purpose of symmetrical canyon and arch thickening from crown to abutment, the shape of the horizontal section of a parabolic arch dam is determined by the following two parabolas:

At the upstream face of the dam:

$$y_u(x,z) = \frac{1}{2r_u(z)}x^2 + b(z) \tag{18}$$

At the downstream face of the dam:

$$y_d(x,z) = \frac{1}{2r_d(z)}x^2 + b(z) + t_c(z) \tag{19}$$

where r_u and r_d are radii of curvatures correspond to upstream and downstream curves respectively, and functions of nth order with respect to z can be used for those radii:

$$r_u = \sum_{i=1}^{n} L_i r_{ui} \qquad r_d = \sum_{i=1}^{n} L_i r_{di} \tag{20}$$

where r_{ui} and r_{di} are the values of r_u and r_d at the ith level, respectively.

4. The Finite Element Model of an Arch Dam

One double curvature arch dam (Morrow Pint) is analyzed to assist the validation of the finite element model utilized in this study. This dam has been studied by many researchers, so the results can be verified with already published material. This dam is located on the Gunnison River in Montrose Country near the village of Cimmaron, Colorado. The dam is 142 m high with a crest length of 221 m and is 3.6 m thick at the crest and 15.8 m thick at the base. The geometric properties of the dam in details can be found in Hall and Chopra (1983).

The physical and mechanical properties involved here are the concrete density (2483 N.s^2/m^4), the concrete poison's ratio (0.2) and the concrete elasticity (27580×10^4 MPa). In this analysis, dam-foundation interaction is omitted, and assuming incompressibility of the fluid, the generalized Westergaard (1933) method is used for dam reservoir interaction. The dam body is discretized with 616 eight-node solid elements (Fig. 3), and each node has three degree of freedom: translations in the nodal x, y and z directions. The arch dam is analyzed as a 3D-linear structure.

The natural frequencies from the other literature and the present work are provided in Table 1. It can be observed that a good conformity has been achieved between the results of the present work with those of the reported in the literature.

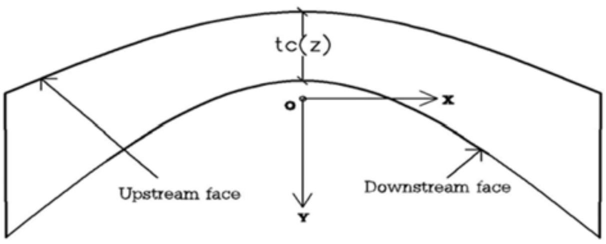

Fig. 2. The Shape of the Horizontal Section of a Parabolic

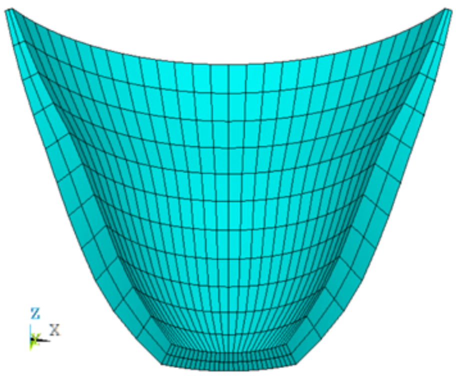

Fig. 3. The Finite Element Model of the Morrow Point Arch Dam

Table 1. Natural Frequencies of the Morrow Point Arch Dam

		Natural frequencies (Hz)			
		Tan & Chopra (1996)		Present work	
Case	Reservoir	Symmetric mode	Antisymmetric mode	Symmetric mode	Antisymmetric mode
1	Empty	4.27	3.81	4.30	3.77
2	Full	2.82	2.91	2.84	3.05

5. Arch Dam Optimization

5.1 Mathematical Model and Optimization Variables

The optimization problem can formally be stated as follows:

$$\begin{aligned} &\text{Find} \quad X = [x_1, x_2, x_3, \ldots, x_n] \\ &\text{tominimizes } Mer(X) = f(X) \times f_{penalty}(X) \\ &\text{subjected to } \; g_i(X) \leq 0, i = 1, 2, \ldots, m \\ &\qquad\qquad x_{imin} \leq x_i \leq x_{imax} \end{aligned} \tag{21}$$

where X is the vector of design variables with n unknowns, g_i is

ith constraint from m inequality constraints and $Mer(X)$ is the merit function; $f(X)$ is the cost; $f_{penalty}(X)$ is the penalty function which results from the violations of the constraints corresponding to the response of the arch dam. Also, x_{imin} and x_{imax} are the lower and upper bounds of design variable vector.

Exterior penalty function method is employed to transform the constrained dam optimization problem into an unconstrained one as follows:

$$f_{penalty}(X) = 1+\gamma_p \sum_{i=1}^{m} \max(0, g_j(x))^2 \tag{22}$$

where γ_p is the penalty multiplier.

5.2 Design Variables

The most effective parameters for creating the arch dam geometry were mentioned in Section 2. The parameters can be adopted as design variables:

$$X = \{s\ \beta\ t_{c1}\ \dots\ t_{cn}\ r_{u1}\ \dots\ r_{un}\ r_{d1}\ \dots\ r_{dn}\} \tag{23}$$

where X is the vector of design variables containing $3n+2$ shape parameters of the arch dam.

5.3 Design Constraints

Design constraints are divided into some groups including the behavioral, geometrical and stability constraints. In most of the existing studies, the separate restrictions of the principal stresses were considered as behavior constraints. In this study, the behavior constraints are defined to prevent the crash and crack of each element (e) of the arch dam under specified safety factor (sf) in all time points of the specified earthquake. For this purpose, the failure criterion of concrete of Willam and Warnke (1975) due to a multi-axial stress state is employed. Thus, time dependent (t) behavior constraints for the dam body are expressed as:

$$\left(\frac{f_p}{f_c}\right)_{e,t} \le \left(\frac{sur}{sf}\right)_{e,t} \Rightarrow gbe(x,t) = \left(\frac{f_p}{f_c} - \frac{sur}{sf}\right)_{e,t} \le 0, e=1,\dots,n_e, t=1,\dots,T \tag{24}$$

where f_p is a function of the principal stress state ($\sigma_1 \ge \sigma_2 \ge \sigma_3$) and sur is the failure surface expressed in terms of principal stresses, uniaxial compressive strength of concrete (f_c), uniaxial tensile strength of concrete (f_t), and biaxial compressive strength of concrete (f_{cb}). In the above relationship, T is the earthquake duration. According to four principal stress states compression-compression-compression, tensile-compression-compression, tensile-tensile-compression, and tensile-tensile-tensile-the failure of concrete is categorized into four domains. In each domain, independent functions describe f_p and the failure surface sur. For instance, in the compression-compression-compression regime f_p and sur are defined as:

$$f_p = \frac{1}{\sqrt{15}}[(\sigma_1-\sigma_2)^2+(\sigma_1-\sigma_3)^2+(\sigma_2-\sigma_3)^2]^{\frac{1}{2}} \tag{25}$$

$$sur = \frac{2r_2(r_2^2-r_1^2)\cos\eta + r_2(2r_1-r_2)[4(r_2^2-r_1^2)cos^2\eta+5r_1^2-4r_1r_2]^{\frac{1}{2}}}{4(r_2^2-r_1^2)cos^2\eta+(r_2-2r_1)^2} \tag{26}$$

where the angle of similarity $0 \le \eta \le 60$ describes the relative magnitudes of the principal stresses as:

$$\cos\eta = \frac{2\sigma_1-\sigma_2-\sigma_3}{\sqrt{2}[(\sigma_1-\sigma_2)^2+(\sigma_1-\sigma_3)^2+(\sigma_2-\sigma_3)^2]} \tag{27}$$

The parameters r_1 and r_2 represent the failure surface of all the stress states with $\eta = 0$ and $\eta = 60$, respectively, and these are functions of the principal stresses and concrete strengths (fc, ft , fcb). The details of the failure criterion can be found in Willam and Warnke (1975). Therefore, Eq. (24) is checked at the center of all dam elements (ne) with a safety factor chosen as $sf = 1$ for the earthquake loading (US Bureau of Reclamation 1977). If it is satisfied, there is no cracking or crushing. Otherwise, the material will crack if any principal stress is tensile, while crushing will occur if all principal stresses are compressive.

The most important geometrical constraints are those that prevent from intersection of upstream face and downstream face as:

$$r_{dn} \le r_{un} \Rightarrow \frac{r_{dn}}{r_{un}} - 1 \le 0,\ n=1,\dots,n \tag{28}$$

where r_{dn} and r_{un} are the radii of curvatures at the down and upstream faces of the dam in the nth position in z direction. The geometrical constraint that is applied to facilitate the construction is defined as:

$$s \le s_{all} \Rightarrow \frac{s}{s_{all}} - 1 \le 0 \tag{29}$$

where s is the slope of overhang at the downstream and upstream faces of dam and s_{all} is its allowable value. Usually s_{all} is taken as 0.3 (see Zhu *et al.*, 1992).

5.4 Objective Function

The objective function is the construction cost or volume of concrete of the dam. The construction cost may be expressed as:

$$f(X) = p_v v(X) + p_a a(X) \tag{30}$$

where X is the design variable vector, $v(X)$ and $a(X)$ are the concrete volume and the casting area of dam body, respectively. The unit price of the concrete and casting are chosen as p_v = \$33.34 and p_a = \$6.67, respectively.

The volume of the concrete can be determined by integrating from dam surfaces as:

$$v(X) = \iint_{Area} |y_d(x,z) - y_u(x,z)| dxdz \tag{31}$$

in which, *Area* is an area produced by projecting of dam on xz plane. The areas of the casting can approximately be calculated by summing the areas of the upstream and downstream faces as follows:

$$\begin{aligned} a(X) &= a_u(X) + a_d(X) \\ &= \iint_{Area} \sqrt{1+\left(\frac{dy_u}{dx}\right)^2+\left(\frac{dy_u}{dx}\right)^2} dxdz + \iint_{Area} \sqrt{1+\left(\frac{dy_d}{dx}\right)^2+\left(\frac{dy_d}{dx}\right)^2} dxdz \end{aligned} \tag{32}$$

where a_u and a_d are the casting areas of upstream and downstream faces, respectively (Seyedpoor and Gholizadeh (2008)).

To evaluate $v(X)$ and $a(X)$, a computer program is prepared using the MATLAB (2003).

6. Numerical Examples

In order to assess the effectiveness of the proposed procedure, two double curvature arch dams are selected to verify the efficiency of the new optimization algorithms. A finite element model based on time history analysis is presented for the double-curvature arch dam. The arch dam is treated as a three dimensional linear structure. To mesh of the arch dam body, an eighty-node isoperimetric solid element is used. It is assumed that the dam foundation is rigid to avoid the extra complexities that would otherwise arise. The material properties of the dam are given in Table 2. Specifications of the CSS, PSO and CSS-PSO methods are provided in Tables 3 to 5.

In the analysis phase, the linear dynamic analysis of the system is performed using the Newmark time integration method. Two cases are considered for these arch dams:

Case 1: The reservoir is considered empty. The load involved here are gravity and earthquake load.

Case 2: The reservoir is considered full. The load involved here are gravity load, hydrostatic and hydrodynamic pressures, and earthquake load.

To evaluate the stress components at center of dam elements a computer program is coded using Opensees (2011). The structural damping in the system is included by using a Rayleigh type of damping matrix given by:

$$C_s = \alpha K_s + \beta M_s \tag{33}$$

Where M_s, C_s and K_s are the structural mass, damping and stiffness matrices, respectively. α and β are variable factors to obtain a desirable damping in the system. In many practical structural problems, the mass damping may be ignored and then

Table 2. The Material Properties of the Arch Dam

Elastic modulus of concrete	27580×10^4 MPa
Concrete poison's ratio	0.2
Mass density of concrete	2483 kg/m^3
Uniaxial compressive strength of the concrete	30 MPa
Uniaxial tensile strength of the concrete	3 MPa
Biaxial compressive strength of the concrete	36 MPa

Table 3. Specifications of the Charged System Search (CSS) Method

Parameter	Specification
Number of CPs	Number of variable
Max acceleration coefficient	1.00
Max velocity coefficient	0.50
Min acceleration coefficient	0.50
Min velocity coefficient	0.00
Magnitude of a	1.00
Maximum iterations	100.00

Table 4. Specifications of the Particle Swarm Optimization (PSO) Method

Parameter	Specification
Swarm size	Number of variable
Cognitive parameter	2.00
Social parameter	2.00
Max inertia weight	0.80
Min inertia weight	0.40
Maximum iterations	100.00

Table 5. Specifications of the Particle Swarm Optimization (CSS-PSO) method

Parameter	Specification
Swarm size	Number of variable
Cognitive parameter	1.50
Social parameter	1.50
Max velocity coefficient	0.80
Min velocity coefficient	0.40
Max acceleration coefficient	1.00
Min acceleration coefficient	0.50
Maximum iterations	100.00

the structural damping can be calculated as:

$$C_s = \frac{\xi}{\pi f} K_s \tag{34}$$

where f is the main frequency of the structure and f is a damping ratio. In the present study $\xi = 0.1$ is considered.

6.1 Morrow Point Arch Dam

In this example, the optimization of Morrow Point arch dam is performed. For this test example, the volume of concrete is taken as the objective function. To create the dam geometry, three fifth-order functions are considered for $t_c(z)$, $r_u(z)$, and $r_d(z)$. Thus, by accounting for two shape parameters needed to define the curve of upstream face $b(z)$, the dam is modeled by 20 shape design variables as:

$$X = \{s\ \beta\ t_{c1}\ t_{c2}\ t_{c3}\ t_{c4}\ t_{c5}\ t_{c6}\ r_{u1}\ r_{u2}\ r_{u3}\ r_{u4}\ r_{u5}\ r_{u6}\ r_{d1}\ r_{d2}\ r_{d3}\ r_{d4}\ r_{d5}\ r_{d6}\} \tag{35}$$

The lower and upper bounds of design variables required for the optimization process are determined using a preliminary design method (Varshney, 1982):

$$\begin{array}{llll} 0 \le s \le 0.3 & 3 \le t_{c1} \le 10 & 100 \le r_{u1} \le 135 & 100 \le r_{d1} \le 135 \\ 0.5 \le \beta \le 1 & 5 \le t_{c2} \le 15 & 85 \le r_{u2} \le 115 & 85 \le r_{d1} \le 115 \\ & 10 \le t_{c3} \le 20 & 70 \le r_{u3} \le 100 & 70 \le r_{d1} \le 100 \\ & 15 \le t_{c4} \le 25 & 60 \le r_{u4} \le 80 & 60 \le r_{d4} \le 80 \\ & 20 \le t_{c5} \le 30 & 45 \le r_{u5} \le 60 & 45 \le r_{d5} \le 60 \\ & 25 \le t_{c6} \le 35 & 30 \le r_{u6} \le 45 & 30 \le r_{d6} \le 45 \end{array} \tag{36}$$

The El Centro N–S record of the Imperial Valley earthquake of 1940 is chosen as the ground motion (Pacific Earthquake Engineering Research Center, 2005). The selected earthquake has a duration of 30s. Also, the peak acceleration of the record is

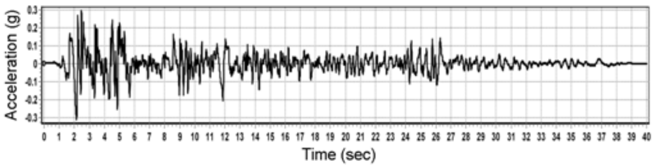

Fig. 4. The El Centro N–S Record of the 1940 Imperial Valley Earthquake

nearly 0.313 g. The record shown in Fig. 4 is applied to the arch dam system in the upstream direction.

Table 6 represents the design vectors and the volume of thearch dam obtained by different methods. It can be seen that CSS-PSO leads to better results than both CSS and PSO. Fig. 5 shows the convergence curves for three methods for the optimum design of the arch dam in Case 1. As it can be seen, not only the convergence rate of the CSS-PSO is higher than the standard methods, but also the accuracy of this method is better. Optimum shapes of the arch dam obtained by various methods are schematically shown in Fig. 6. It can be seen that the shape of the arch dam obtained by the CSS-PSO is more uniform than those of the other methods.

6.2 Hypothetical Model

As the second example, a well-known benchmark problem in the field of shape optimization of the arch dam is considered, with the height of 180 m. The width of the valley in its bottom and top sections are 40 m and 220 m, respectively (Fig. 7). For this test example, the construction cost is the objective function.

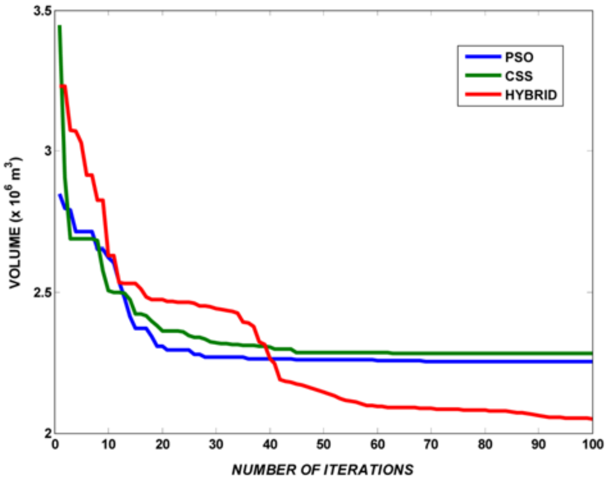

Fig. 5. The Convergence Curves for the PSO, CSS and the Hybrid PSO-CSS (Case 1)

The dam is modeled by 14 shape design variables as:

$$X = \{S \;\; \beta \;\; t_{c1} \;\; t_{c2} \;\; t_{c3} \;\; t_{c4} \;\; r_{u1} \;\; r_{u2} \;\; r_{u3} \;\; r_{u4} \;\; r_{d1} \;\; r_{d2} \;\; r_{d3} \;\; r_{d4}\} \qquad (37)$$

The lower and upper bounds of the design variables are considered using empirical design methods of Varshney (1982):

$$\begin{array}{llll} 0 \le s \le 0.3 & 4 \le t_{c1} \le 12 & 50 \le r_{u1} \le 180 & 50 \le r_{d1} \le 180 \\ 0 \le \beta \le 1 & 8 \le t_{c2} \le 25 & 40 \le r_{u2} \le 120 & 40 \le r_{d2} \le 120 \\ & 10 \le t_{c3} \le 35 & 15 \le r_{u3} \le 50 & 15 \le r_{d3} \le 50 \\ & 12 \le t_{c4} \le 40 & 10 \le r_{u4} \le 40 & 10 \le r_{d4} \le 00 \end{array} \qquad (38)$$

Table 6. Optimum Designs of the Arch Dam Obtained by Different Methods

	Case 1			Case 2		
Variable No.	PSO	CSS	Hybrid CSS & PSO	PSO	CSS	Hybrid CSS & PSO
S	0.1324	0.0768	0.1500	0.1997	0.2183	0.2978
β	0.6547	0.7284	0.9140	0.9888	0.9744	0.9983
t_{c1}	5.6203	5.1907	2.9741	6.8690	6.2301	6.0086
t_{c2}	4.9422	5.7642	4.9892	14.2055	15.0000	13.1002
t_{c3}	10.4619	9.9736	10.0153	17.5240	17.8633	15.2319
t_{c4}	15.0628	15.1453	14.9812	21.7109	20.5649	24.6122
t_{c5}	20.1605	22.2487	19.9789	23.5017	25.7853	20.0053
t_{c6}	31.4099	26.5918	26.4647	28.6766	26.9561	25.0028
r_{u1}	124.0109	111.4046	119.5898	133.9955	129.1776	133.4167
r_{u2}	105.348	91.5467	106.1840	92.5018	109.5474	104.8836
r_{u3}	91.4923	90.9165	93.9875	99.9468	82.1169	87.4033
r_{u4}	73.9849	76.7320	73.1835	74.6562	70.8406	78.5695
r_{u5}	56.7679	53.4083	57.6895	50.6424	59.9997	53.6063
r_{u6}	40.9305	38.5734	33.1584	42.9266	40.3869	39.8787
r_{d1}	107.6258	110.0734	111.8234	112.3219	117.8332	101.8954
r_{d2}	105.244	88.4880	106.0160	85.0033	85.5730	85.6888
r_{d3}	81.7535	80.8677	93.9742	70.6935	73.1176	70.2540
r_{d4}	73.9410	72.5760	72.9709	65.0838	64.2909	60.9596
r_{d5}	56.7811	48.4788	57.4853	50.5577	54.0687	52.1588
r_{d6}	35.5770	30.6391	33.0940	39.4978	35.5311	38.1512
Concrete volume (m^3) (10^5)	2.25	2.28	2.04	3.49	3.47	3.36

Fig. 6. Optimum Shapes of the Arch Dam Obtained by Different Methods: (a) PSO, (b) CSS, (c) Hybrid PSO-CSS

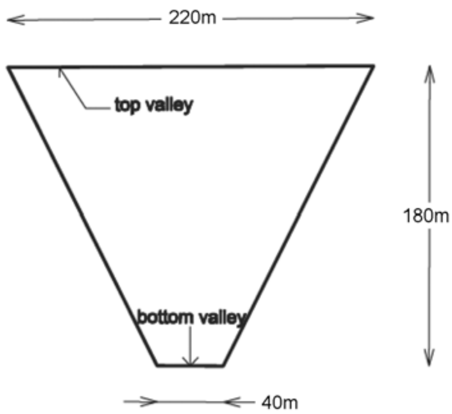

Fig. 7. The Valley Dimensions of the Arch Dam

Table 7 represents the design vectors and costs of the arch dam obtained by different methods. It can be seen that the CSS-PSO provides a better results than both CSS and PSO. Fig. 8 shows the convergence curves for three methods for the optimum design of arch dam in Case 2.

7. Parametric Study

In the design process, water depth and earthquake intensity are evaluated based on the hydrological and seismic studies in the dam region, respectively. In this section a parametric study for the second example is performed to investigate the effect of water depth and earthquake intensity on the cost optimization of the arch dams. Table 8 summarizes the water depths, the earthquake intensities considered and the results obtained in this case study using the CSS-PSO algorithms. The earthquake intensity is considered utilizing the peak ground acceleration (PGA) of the record. Earthquake intensity of PGA = 0.313 g and PGA = 0.45 g is the El Centro record by unity and $\frac{0.45}{0.313} = 1.437$ scale factor, respectively. The water depth is considered from bottom valley, and is equal to 0 and 180 for the empty and full reservoirs, respectively. It can be seen that the construction cost of the arch dam increases with both the water depth and the earthquake intensity.

Table 7. Optimum Designs of the Arch Dam Obtained by Different Methods

	Case 1			Case 2		
Variable No.	PSO	CSS	Hybrid CSS-PSO	PSO	CSS	Hybrid CSS-PSO
S	0.2391	0.2537	0.1568	0.3000	0.0729	0.2994
β	0.7526	0.7057	0.7691	0.8442	0.6617	0.9993
t_{c1}	8.2785	10.2484	4.8434	5.1497	8.4340	7.9252
t_{c2}	16.9436	11.332	12.0562	24.9982	17.5300	12.4397
t_{c3}	13.754	24.4834	10.4478	20.3836	18.9079	18.5096
t_{c4}	34.9647	30.6733	14.9583	16.2745	22.6661	13.9388
r_{u1}	108.9378	118.5608	151.5834	120.3613	157.4936	160.1748
r_{u2}	56.3254	62.8361	69.5997	77.2102	108.6227	103.899
r_{u3}	31.6012	36.9318	38.0772	35.2023	43.2428	41.9721
r_{u4}	33.0529	39.0636	33.2699	33.8541	19.8586	35.2535
r_{d1}	104.6383	102.0752	128.9585	50.8117	50.0000	51.1989
r_{d2}	50.2002	62.747	67.1517	40.6808	40.8569	40.1239
r_{d3}	31.5986	35.2232	27.0705	29.2908	20.1374	25.9333
r_{d4}	22.7025	27.5876	27.4823	31.0018	17.6255	20.2469
Cost of the dam ($\$10^7$)	1.36	1.28	1.00	2.45	2.57	2.23

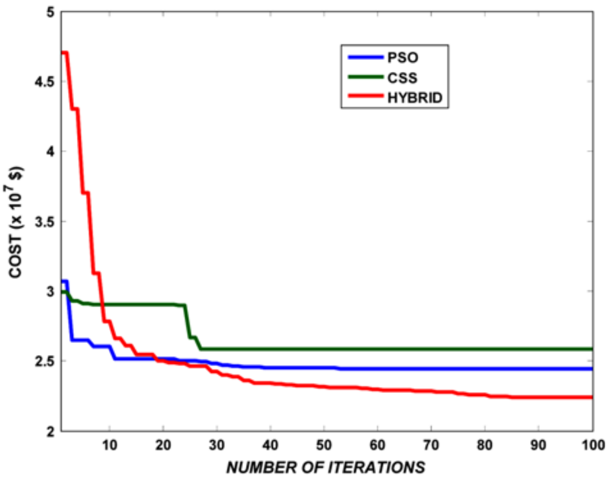

Fig. 8. The Convergence Curves for the PSO, CSS and Hybrid PSO-CSS Algorithms (Case 2)

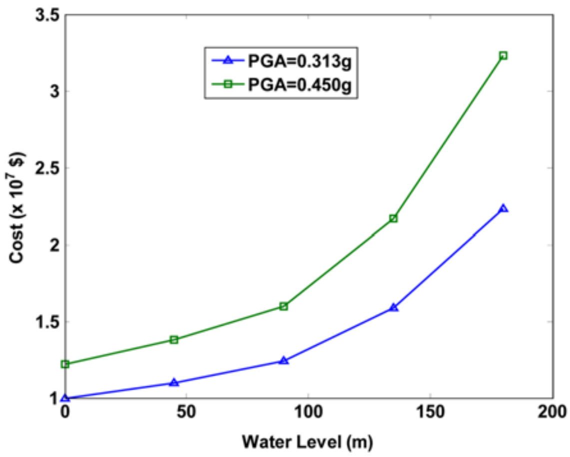

Fig. 9. Optimal Construction Cost of the Arch Dam

Table 8. Results of the Parametric Study

Earthquake intensity	Water depth (m)	Construction cost of the dam ($\$10^7$)
PGA = 0.313 g	0	1.00
	45	1.10
	90	1.24
	135	1.59
	180	2.23
PGA = 0.45 g	0	1.22
	45	1.38
	90	1.50
	135	2.17
	180	3.23

Figure 9 shows the curves representing the variations between the optimal construction cost and the water depth under two different earthquake intensities. The curves have the same non-linear trend and in both cases the cost increases with the water depth. Also, in the case of earthquake with higher intensity, the construction cost is increased quite rapidly because of the increase of the hydrodynamic pressure due to the increase the water depth.

8. Conclusions

In this paper, the shape optimization of two double-curvature arch dams is performed under seismic loading. The volume and cost of the arch dam (including the concrete volume and the casting areas) are considered as the objective function, with stress, geometrical and stability constraints. The generalized Westergaard method is utilized for dam reservoir interaction. In order to validate the finite element model, the Morrow Point arch dam is analyzed.

For optimizing the arch dams, three meta-heuristic algorithms, namely the CSS, PSO and hybrid CSS and PSO are utilized. From the results of this study it can be seen that the CSS-PSO leads to better results than both standard CSS and PSO. Also, the convergence rate of the CSS-PSO is higher than those of the standard methods. The shape of the arch dam obtained by the CSS-PSO is more uniform than those of the other methods. In the last section, a parametric study is performed in order to illustrate the effect of the water depth and earthquake intensity on the optimal construction cost of the arch dam. It can be seen that in the higher earthquake intensities, the optimal construction cost is increased considerably by the increase of the water depth.

Acknowledgements

The first author is grateful to the Iran National Science Foundation for the support.

References

Eberhart, R.C. and Kennedy, J. (1995). "A new optimizer using particle swarm theory." *Proceedings of the Sixth International Symposium on Micro Machine and Human Science*, Nagoya, Japan.

Fialho, J. F. L. (1955). *Leading principles for the design of arch dams – A new method of tracing and dimensioning*, LNEC, Lisbon, Portugal.

Gholizadeh, S., and Seyedpoor, S. M. (2011). "Optimum design of arch dams for frequency limitations." *International Journal of Optimization in Civil Engineering* Vol. 1, pp. 1-14.

Hall, J. F. and Chopra, A. K. (1983). "Dynamic analysis of arch dams including hydrodynamic effects." *Journal of Engineering Mechanics, ASCE*, Vol. 109, No. 1, pp. 149-167.

Kaveh, A. and Talatahari, S. (2010a). "A novel heuristic optimization method: Charged system search." *Acta Mechanica*, Vol. 213, Nos. 3-4, pp. 267-289.

Kaveh, A. and Talatahari, S. (2010b). "Optimal design of truss structures via the charged system search algorithm." *Structural Multidisciplinary Optimization*, Vol. 37, No. 6, pp. 893-911.

Kaveh, A. and Talatahari, S. (2010c). "Charged system search for optimum grillage systems design using the LRFD-AISC code." *Journal of Constructional Steel Research*, Vol. 66, No. 6, pp. 767-771.

Kaveh, A. and Talatahari, S. (2011). "Optimization of large-scale truss structure using modified charged system search." *International Journal of Optimization in Civil Engineering*, Vol. 1, No. 1, pp. 15-28.

MATLAB (2009). *The language of technical computing*, Math Works Inc.

McKenna, F., Fenves, G. L., and Scott, M. H. (2003). *Open system for earthquake engineering simulation*, Pacific Earthquake Engineering Research Center, University of California, Berkeley, USA.

Mohr, G. A. (1979). "Design of shell shape using finite elements." *Computers and Structures*, Vol. 10, No. 5, pp. 745-749.

Rajan. M. K. S. (1968). *Shell theory approach for optimization of arch dam shapes*, PhD Thesis, University of California, Berkeley, USA.

Ricketts, R. E. and Zienkiewicz, O. C. (1975). S*hape optimization of concrete dams, criteria and assumptions for numerical analysis of dams*, Quadrant Press, Swansea, London, UK.

Seyedpoor, S. M. and Gholizadeh, S. (2008). "Optimum shape design of arch dams by a combination of simultaneous perturbation stochastic approximation and genetic algorithm." *Advances in Structural Engineering*, Vol. 11, No. 5, pp. 501-510.

Sharma, R. L. (1983). *Optimal configuration of arch dams*, PhD Thesis, Indian Institute of Technology, Kanpur, India.

Sharpe, R. (1969). *The optimum design of arch dams*, Institution of Civil Engineers, UK.

Tan, H. and Chopra, A. K. (1996). "Dam-foundation rock interaction effects in earthquake response of arch dams." *ASCE, Journal of Structural Engineering*, Vol. 122, No. 5, pp. 528-538.

Varshney, R. S. (1982). *Concrete dams*, Second Ed., Oxford and IBH Publishing Co., New Delhi, India.

Westergaard, H. M. (1933). "Water pressure on dams during earthquakes." *Transactions of the American Society of Civil Engineering*, Vol. 98, No. 2, pp. 418-433.

Willam, K. J. and Warnke, E. D. (1975). "Constitutive model for the tri-axial behavior of concrete." *Proceedings of the International Association for Bridge and Structural Engineering*, ISMES, Bergamo, Italy, Vol. 19, p. 174.

Zhu, B., Rao, B., Jia, J., and Li, Y. (1992). "Shape optimization of arch dam for static and dynamic loads." *J Struct Eng,* ASCE, Vol. 118, No. 11, pp. 2996-3015.